

# Single-Factor Comprehensive Reservoir Quality Classification Evaluation—Taking the Hala’alat Mountains at the Northwestern Margin of the Junggar Basin as an Example

Qiongyao Pu, Jun Xie, XinShuai Li, YuanPei Zhang, Xiao Hu,\* Xiaofan Hao, Fengrui Zhang, Zhengquan Zhao, Jianfeng Cao, Yan Li, and Renjie Gao



Cite This: *ACS Omega* 2023, 8, 37065–37079



Read Online

ACCESS |

Metrics & More

Article Recommendations

**ABSTRACT:** In the process of petroleum geology exploration and development, reservoir quality evaluation is an essential component. However, conventional reservoir quality evaluation methods are no longer able to provide accurate and comprehensive assessments for all types of reservoirs. Therefore, the comprehensive evaluation of reservoir quality using multiple single factors is of significant importance in improving the level of reservoir quality assessment and enhancing the effectiveness of oil and gas exploration techniques. Conventional reservoir quality evaluation methods can assess only the quality of individual reservoir properties, resulting in limited classification outcomes. Taking the Cretaceous formations in the southern margin of the Hala’alat Mountain in the Junggar Basin as the research object, preliminary classification criteria were established based on the principles of formation coefficient, storage coefficient, and flow unit index. Combining experimental data such as core observation, thin-section identification, pore permeability analysis, and scanning electron microscopy, a comprehensive set of reservoir quality classification and evaluation criteria were developed. Furthermore, the corresponding reservoir classification evaluation maps were generated to illustrate the spatial distribution of reservoir quality. The study reveals that the area can be classified into four types of reservoirs, namely, Class I, Class II, Class III, and Class IV, corresponding to the best reservoir, relatively good reservoir, relatively poor reservoir, and poor reservoir, respectively. Among them, the second ( $K_1q_2$ ) and third ( $K_1q_3$ ) members of the Cretaceous Qingshuihe Formation, as well as the first ( $K_1h_1$ ) and third ( $K_1h_3$ ) members of the Cretaceous Hutubi Formation, exhibit the best reservoir quality as Class II. On the other hand, the second member of the Cretaceous Hutubi Formation ( $K_1h_2$ ) exhibits the best reservoir quality as Class III, with relatively poorer reservoir quality overall. The research findings of this study can provide an important theoretical basis for oil and gas exploration and development in the region.

## 1. INTRODUCTION

In the exploration stage, qualitative evaluation of reservoirs is widely utilized. Due to limited regional data, reservoir evaluation and classification are often conducted based on parameters such as porosity, permeability, and pore structure.<sup>1</sup> The results of qualitative evaluation are preliminary and approximate,<sup>2</sup> and various indicators related to lithology, facies, petrophysical properties, electrical properties, oil saturation, diagenesis, pore structure, and heterogeneity are involved in reservoir classification evaluation. Loucks et al. established a database encompassing various measurements of porosity and permeability accuracy in order to comprehend the matrix reservoir quality of the Austin Chalk Formation. They also compared the advantages and disadvantages of various single-factor methods for evaluating reservoir quality.<sup>3</sup> In order to enhance the accuracy of reservoir quality evaluation, Liu et al. utilized a machine learning method called gradient boosting decision tree (GBDT) algorithm to design and perform reservoir quality classification assessment.<sup>4</sup> Jiang et al. employed an optimized clustering algorithm to provide a more accurate classification scheme for low-permeability tight reservoirs.<sup>5</sup> In order to accurately evaluate the impact of volcanic rock alteration on reservoir quality in the Songliao

Basin, Pan et al. established a reservoir quality evaluation method based on conventional well logging.<sup>6</sup> To address the classification problem of tight sandstone reservoirs with limited experiential information and core experiments, Xie et al. proposed a comprehensive classification method based on a principal component analysis fuzzy clustering means. This method effectively classified reservoir quality by utilizing flexible membership degrees.<sup>7</sup> Ren et al. established a K nearest neighbor (KNN) classification template based on the principles of cluster analysis. By analyzing the discrimination results of reservoir types and their corresponding reservoir quality classifications, they evaluated the contribution of various reservoir types to oil and gas production and verified the reliability of reservoir type classification.<sup>8</sup> In addition, Shalaby et al. evaluated the quality of sandstone reservoirs in

Received: June 22, 2023

Accepted: September 18, 2023

Published: September 28, 2023



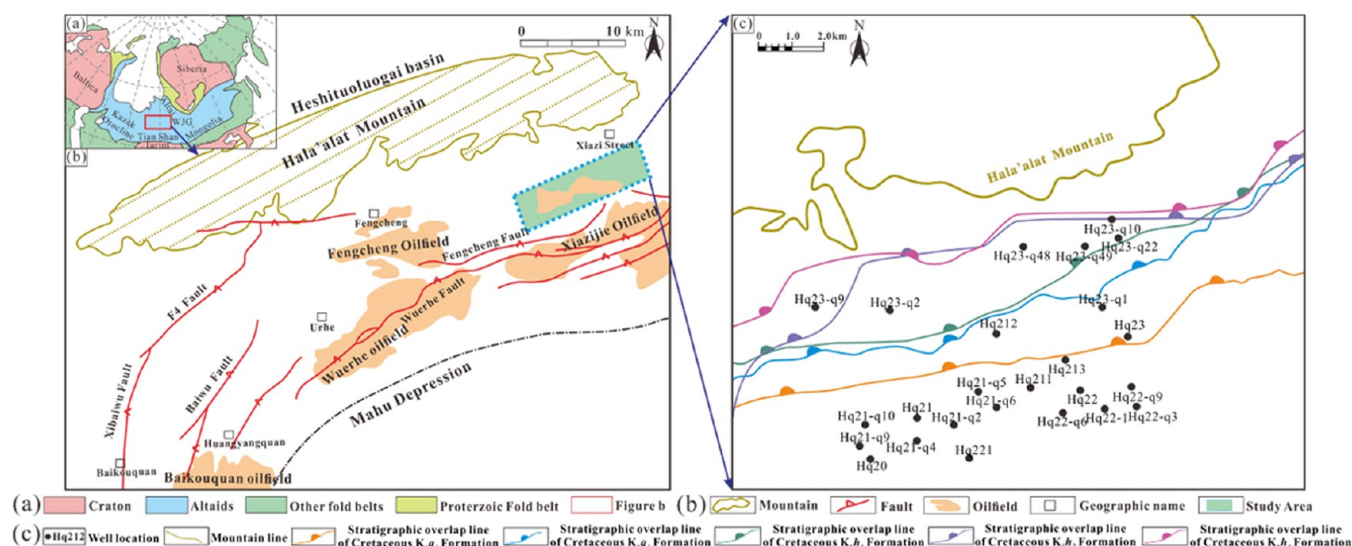


**Figure 1.** Regional structure and composite strata in the study area. (a) Simplified map of northwestern Eurasia, indicating the Altai and the location of West Junggar (WJG) within the inset, modified after Choulet et al.;<sup>19</sup> (b) tectonic map of the WJG Mountains; and (c) well location map in the study area.

the Carboniferous Permian Cooper Basin of South Australia, using a combination of rock physics, facies analysis, sedimentology, and well log interpretation. These multifactor evaluations provided a comprehensive assessment of the reservoir quality of the Kurrajong Formation.<sup>9</sup> In general, quantitative reservoir evaluation involves the comprehensive assessment of multiple factors that influence reservoir properties, based on the selection of reservoir evaluation parameters. This process results in the derivation of a comprehensive evaluation index, which is then used to classify reservoirs.<sup>10</sup>

The single-factor comprehensive reservoir quality evaluation method refers to the separate calculation of the individual factors that affect reservoir quality. Commonly used methods include principal component analysis and the comprehensive scoring method. These methods are then combined to provide a comprehensive evaluation of reservoir quality.<sup>10</sup> For instance, Li Shengbiao investigated the reservoir characteristics in the Wangji Oilfield of Henan Province. Based on the classification evaluation using static reservoir data, Li proposed a comprehensive evaluation of the reservoir using three different single-factor methods: storage coefficient, stratigraphic coefficient, and flow zone index. This approach helped establish the reservoir classification evaluation criteria.<sup>11</sup> Shasha et al. conducted key single-factor evaluations of reservoir quality using storage coefficient, stratigraphic coefficient, and flow zone index and established corresponding reservoir classification criteria.<sup>12</sup> Li et al. classified the reservoirs of a deepwater gas field in Hainan using flow unit index, providing an approach for reservoir evaluation and improving the interpretational accuracy of reservoir parameters to a certain extent.<sup>13</sup> Liu et al. utilized SPSS statistical analysis software to discern the ability of flow units and the correlations among various attribute parameters representing the reservoir. They investigated the application of multiple parameter flow units in reservoir evaluation.<sup>14</sup> In summary, the single-factor comprehensive reservoir quality evaluation method is a practical approach that can accurately assess reservoir quality. It provides a scientific basis and technical support for oil and gas exploration and development.

The study area is located on the western uplift of the northwestern margin of the Junggar Basin, in the southern slope zone of the Hala'alat Mountains.<sup>15</sup> It is one of the important oil and gas production bases in China. The region has a widespread distribution of Cretaceous reservoirs and abundant oil and gas resources. However, previous exploration efforts in the area were limited, and the area is still in the early stage of exploration. A detailed study of reservoir quality evaluation has not been conducted, which severely hampers the progress of future exploration and development in the study area. Therefore, the characterization and quality classification evaluation of reservoirs in this area are urgent issues that must be addressed. This study takes the Cretaceous reservoirs in the Hala'alat Mountains, located in the northern margin of the Junggar Basin, as an example to explore the application of the single-factor comprehensive reservoir quality evaluation method. It aims to provide references and assistance for oil and gas exploration and development in the region as well as to provide a scientific basis for future exploration and development work. This has significant strategic implications for ensuring energy supply security and promoting economic development in our country.

## 2. GEOLOGICAL SETTINGS

The Hala'alat Mountain area is located at the leading edge of the thrust fold belt of the Hala'alat Mountain, which is situated on the northern margin of the Junggar Basin. It borders the Uxia Fault Step Zone and the northern slope zone of the Mahu Depression toward the interior of the Junggar Basin. It is closely adjacent to the southern part of the Mahu Depression and is bounded by the Darbut Fault to the north, where it connects with the Heshituoluogai basin.<sup>16</sup> The western boundary is formed by the Zayier Mountains, while the eastern boundary is the Shixi Depression. The favorable exploration area covers approximately 1000 km<sup>2</sup>.<sup>17</sup> The slope zone above the thrust sheet of Hala'alat Mountain is overlain by Mesozoic strata. The study area is located structurally on the western uplift of the northwestern margin of the Junggar Basin, within the southern slope zone of the Hala'alat

Mountain structure. Overall, it exhibits a northeast southwest orientation in its distribution<sup>18</sup> (Figure 1).

### 3. MATERIALS AND METHODS

**3.1. Materials.** The rock composition data, whole-rock mineralogical X-ray diffraction data, clay mineral X-ray diffraction data, saturation data, as well as reservoir porosity and permeability data used in the study area were collected from Shengli Oilfield Branch of China Petroleum & Chemical Corporation. Porosity and permeability were measured using the 3020 062 helium porosimeter and GDS 90F gas permeameter, respectively, at the Shengli Oilfield Research Institute. The measurement of porosity and permeability was conducted in accordance with the national standard GB/T29172 2012. In order to mitigate the gas slippage effect caused by pressure, Kilmer correction was applied. The inlet pressure, plug sample length and diameter, as well as the testing temperature and duration, can affect the permeability values. During sample preparation, utmost care was taken to minimize any deviation in sample length and diameter, and the certainty of permeability values was ensured by extending the testing duration.

This study selected five sublayers ( $q_2$ ,  $q_3$ ,  $h_1$ ,  $h_2$ , and  $h_3$ ) from the Cretaceous section of 25 wells in the Hala'alat Mountain region, located at the northwest margin of the Junggar Basin. A total of 48 reservoir core samples were selected from the core sections of these wells. Each core sample was impregnated with blue epoxy resin under vacuum, resulting in the production of 40 thin sections. These thin sections were used to analyze petrological characteristics, grain structure, pore structure, and visual porosity. Some sections were stained with Alizarin Red S for carbonate mineral identification. The authigenic clay minerals, micropores, and microfractures were studied using scanning electron microscopy (SEM). Mineral grain size, mineral composition, and pore structure analysis of the 40 thin sections were conducted using a Leica polarizing microscope in the Mineral Laboratory of Shandong University of Science and Technology.

**3.2. Methods.** In order to achieve economical and effective development of low- to medium-permeability reservoirs, identifying areas with relatively favorable oil and gas enrichment through a comprehensive reservoir evaluation is critical. The conventional reservoir evaluation approach primarily focuses on classification evaluation, wherein the classification indicators utilized predominantly include lithology, physical properties, pore structure, sedimentary microfacies, oil testing, and production testing. However, due to the constraints posed by practical data acquisition in oil fields, reservoir evaluation, in most cases, is limited to a small number of samples or well points only, with scant theoretical or symbolic significance, hampering our ability to comprehend the planar variation features of the reservoirs from a surface perspective.

To address the limitations discussed in reservoir evaluation, this study has identified three parameters—formation coefficient method, storage coefficient method,<sup>20,21</sup> and flow zone index method—<sup>13,14,22</sup> for conducting a preliminary analysis of the reservoir from diverse aspects. This comprehensive analysis will be based on the outcome of the preliminary examination.

**3.2.1. Formation Coefficient Evaluation Method.** The formation coefficient ( $K_h$ ) evaluation Method is one of the methods used to assess the storage capacity of geological formations.<sup>23–26</sup> It is a quantitative approach to evaluate reservoir quality. The fundamental principle is to evaluate the

variations in the reservoir formation factor, which reflects the changes in reservoir properties and fluid flow characteristics. It refers to the influence of the formation structure and sedimentary environment on reservoir properties and fluid flow. The results vary according to different formation types and characteristics of stored substances. The higher the formation factor ( $K_h$ ), the higher the individual well production of oil wells. Its value can visually identify relatively high-yield oil and gas areas.<sup>27</sup> The equation for it is as follows:

$$K_h = \frac{\theta^*H}{1 - S_w} \quad (1)$$

( $\theta$ : reservoir porosity;  $H$ : the effective reservoir thickness;  $S_w$ : the saturation of water in rocks).

**3.2.2. Storage Coefficient Evaluation Method.** The storage coefficient ( $\Phi_h$ ) evaluation method is a technique used to assess storage capacity. Based on the reservoir's petrophysical parameters and fluid dynamic characteristics, it involves constructing a physical model of the geological reservoir to calculate the reservoir's effective storage volume and fluid driving force, thereby evaluating the storage coefficient of the reservoir.<sup>28</sup> The storage coefficient refers to the ratio of the effective storage volume to the total storage volume of a reservoir and is one of the important indicators for measuring the storage capacity of a reservoir. A larger storage coefficient ( $\Phi_h$ ) indicates a stronger storage capacity of the reservoir, and this coefficient can more intuitively identify favorable oil and gas accumulation areas.<sup>29</sup>

The effective storage volume of a reservoir ( $V_e$ )

$$V_e = A^*h^*\Phi^*S_n \quad (2)$$

The total storage volume ( $V_t$ )

$$V_t = A^*h^*\theta \quad (3)$$

The storage coefficient ( $\Phi_h$ )

$$\Phi_h = \frac{V_e}{V_t} \quad (4)$$

( $V_e$ : the effective storage volume of a reservoir;  $V_t$ : the total volume stored;  $A$ : the effective area of the reservoir;  $h$ : the effective reservoir thickness;  $\Phi$ : the effective porosity of the reservoir;  $S_n$ : the saturation of oil and gas in the reservoir;  $\theta$ : reservoir porosity).

**3.2.3. Flow Unit Evaluation Method.** The flow zone indicator (FZI) analysis method, also known as the flow unit evaluation method, is a technique used to assess rock pore structure and reservoir flow characteristics.<sup>30–32</sup> Section 3.2.3 is an approach that further subdivides reservoir formations using relevant parameters.<sup>33,34</sup> Traditional porosity and permeability interpretation models fit the porosity and permeability values of core samples using an exponential function, resulting in a straight line on logarithmic coordinates.<sup>35–38</sup> Although this model is simple and convenient, it often leads to significant permeability errors in heterogeneous formations. In order to accurately evaluate the permeability parameters of oil and gas fields, extensive research has been conducted by foreign scholars. Altunbay et al. introduced the concept of the average hydraulic unit radius and considered the reservoir pore space as a series of capillaries. By applying Darcy's law, they derived the Kozeny–Carman equation, which characterizes the relationship between the porosity and permeability of different flow

units. Based on the modified Kozeny–Carman equation, the relationship between porosity and permeability can be expressed as follows:

$$K = \frac{1}{F_s \times \tau^2 \times S_{gv}^2} \left[ \frac{\Phi_e^3}{(1 - \Phi_e)^2} \right] = \frac{1}{H_e} \left[ \frac{\Phi_e^3}{(1 - \Phi_e)^2} \right] \quad (5)$$

( $H_e = F_s \times \tau^2 \times S_{gv}^2$ , called the kozenyc constant).

The constant ( $H_e$ ) varies among different flow units but remains a constant value within a specific flow unit.

In order to apply the Kozeny–Carman equation, it is necessary to transform it into a linear equation. By dividing both sides of eq 5 by  $\Phi_e$  and taking the square root, we obtain

$$\sqrt{\frac{K}{\Phi_e}} = \left[ \frac{\Phi_e}{1 - \Phi_e} \right] \frac{1}{\sqrt{F_s \tau S_{gv}}} \quad (6)$$

If the permeability unit is taken as  $\times 10^{-3} \mu\text{m}^2$ , parameters can be defined.

Reservoir quality index (RQI)

$$\text{RQI}(\mu\text{m}) = 0.0314 \times \sqrt{\frac{K}{\Phi_e}} \quad (7)$$

Standardized porosity index ( $\Phi_z$ )

$$\Phi_z = \frac{\Phi_e}{1 - \Phi_e} \quad (8)$$

Flow zone index (FZI)

$$\text{FZI} = \frac{\text{RQI}}{\Phi_z} = 0.0314 \left( \frac{1 - \Phi_e}{\Phi_e} \right) \sqrt{\frac{K}{\Phi_e}} \quad (9)$$

( $K$ : permeability,  $\mu\text{m}^2$ ;  $\Phi_e$ : effective porosity;  $F_s$ : pore geometry index;  $S_{gv}$ : particle surface area per unit particle volume;  $\tau$ : curvature of flow path).

The fundamental principle of this method is to partition the reservoir into flow zones, calculate the parameters such as effective porosity and permeability for each flow zone, and thereby evaluate the petrophysical characteristics and fluid storage of the reservoir. A smaller FZI value indicates a more complex pore structure in the reservoir with a less pronounced relationship between permeability and effective porosity, indicating poorer reservoir fluid flow characteristics. Conversely, a larger FZI value indicates a simpler pore structure in the reservoir, with a more evident relationship between the permeability and effective porosity, indicating better reservoir fluid flow characteristics.

**3.2.4. Comprehensive Reservoir Evaluation Method.** The preceding text utilized the formation coefficient ( $K_h$ ), storage coefficient ( $\Phi_h$ ), and flow zone index (FZI) to quantitatively assess the reservoir, but neither method evaluated the overall characteristics of the reservoir from a certain aspect of its attributes and could not grasp the overall characteristics of the reservoir. These three parameters (formation coefficient, storage coefficient, and flow unit index) are derived from various factors, such as porosity and permeability, to some extent, and thus involve similar controlling factors. These overlaps can produce somewhat similar assessment outcomes, but considering each criterion may emphasize different aspects of reservoir characteristics, such as pore connectivity for the storage coefficient or seepage capacity for the flow unit index, the calculation methods and considerations for each criterion can also vary considerably. Therefore, conducting an integrated

reservoir evaluation is necessary.<sup>29</sup> The comprehensive evaluation of the reservoir in this study is based on the evaluation results of the formation coefficient ( $K_h$ ), storage coefficient ( $\Phi_h$ ), and flow zone index (FZI), comprehensively examining various indicator factors with a focus on revealing the plane distribution pattern of Class A reservoirs, which mainly consist of the evaluation results of each single factor.

In general, a good reservoir corresponds to good storage capacity and flow capacity with relatively low heterogeneity. Based on the evaluation results of the aforementioned individual factors, particularly the intersection set of Class A development, the reservoirs in the study area are classified into four categories: Class I, Class II, Class III, and Class IV (Figure 2).

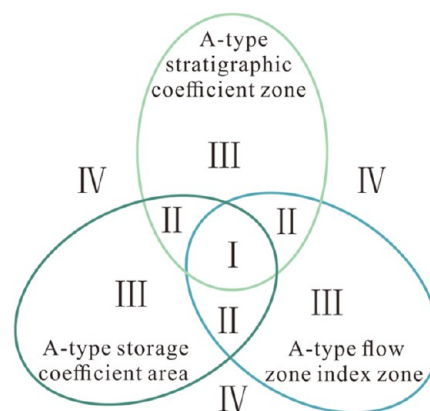


**Figure 2.** Schematic diagram of multifactor comprehensive evaluation method for reservoirs in the study area.

**Class I reservoir:** Refers to reservoirs in which the storage coefficient, formation coefficient, and flow zone index, as evaluated by the key individual factors mentioned earlier, all belong to Class A. This type of reservoir exhibits high porosity and permeability, with thick sand bodies and low heterogeneity. It represents the best reservoir in the study area and serves as a favorable target for hydrocarbon accumulation.

**Class II reservoir:** Refers to the reservoirs where at least two out of the three indicators, namely, storage coefficient, formation coefficient, and flow zone index, belong to Class A. This type of reservoir is relatively good, and hydrocarbon accumulation is also relatively easier in these areas.

**Class III reservoir:** Refers to the reservoirs where at least one out of the three indicators, namely, storage coefficient, formation coefficient, and flow zone index, belongs to Class A. This type of reservoir is relatively poor, and hydrocarbon accumulation is rare in these areas.

**Class IV reservoir:** Refers to the reservoirs where none of the three indicators, namely, storage coefficient, formation coefficient, and flow zone index, belong to Class A. This type of reservoir is considered as a poor reservoir, with minimal hydrocarbon accumulation in these areas.

In summary, an all-inclusive and precise evaluation of reservoir quality incorporating these criteria can efficiently direct exploration and development strategies for oil and gas operations.

## 4. RESULTS

**4.1. Petrological Characteristics.** Conducting reservoir characterization studies to identify high-quality reservoirs is a

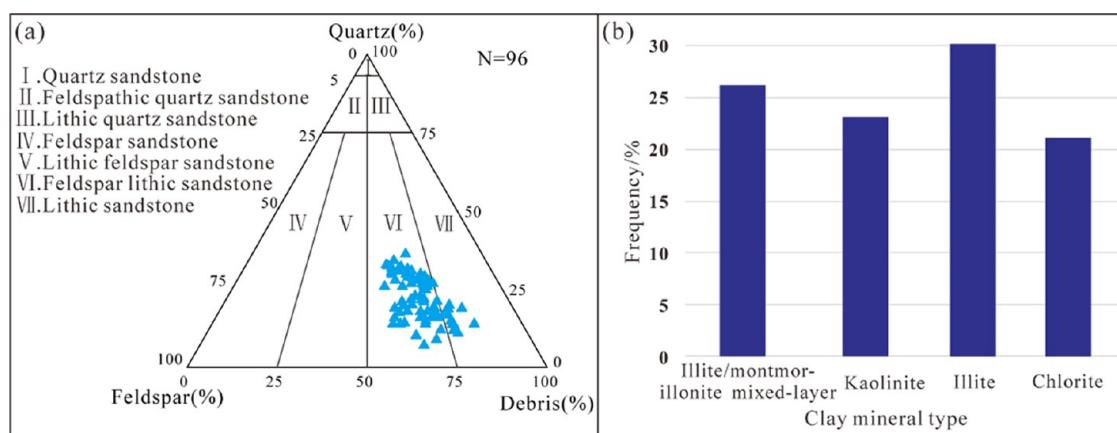


**Figure 3.** Lithology triangle map and clay mineral composition map in the study area. (a) Lithological triangle map; (b) clay mineral type.

key aspect of oilfield exploration and development processes.<sup>39,40</sup> Based on previous studies on the tectonic evolution and provenance analysis of the study area,<sup>41,42</sup> the reservoir characteristics of the study area were investigated by integrating sedimentary features, reservoir petrological characteristics, reservoir properties, pore types, and pore structure characteristics.<sup>43,44</sup> This research provides a basis for reservoir prediction and oilfield development.

Based on core observations and thin-section analysis, the lithology of the Cretaceous reservoir in the study area is predominantly gray, fine-grained feldspathic sandstone, with a minor amount of lithic sandstone (Figure 3a). In the sandstone clasts, the average content of quartz, feldspar, and lithic fragments accounts for 17, 30, and 53%, respectively. The lithic fragments are predominantly composed of sedimentary rocks, with a generally moderate grain sorting. They mainly consist of siltstone, fine-grained sandstone, and mudstone, with a small amount of conglomerate present. The particles are predominantly subangular in shape, with mainly point line contacts between particles and a small amount of concave–convex contacts. The predominant cement type is pore contact cement, with some instances of intergrowth cement. The clay minerals in the reservoir include kaolinite, illite, chlorite, and illite smectite mixed layers, with the highest content of illite. Illite is distributed on grain surfaces, on grain contacts, and within pore throats, forming a localized bridging (Figure 3b).

**4.2. Petrophysical Characteristics.** Based on the analysis of a large number of physical property tests conducted on core samples, the porosity of the Cretaceous sandstone in the study area is predominantly distributed in the range of 10.00–15.00%. The permeability distribution is relatively scattered, with a minimum value of  $0.90 \times 10^{-3} \mu\text{m}^2$  and a maximum value of up to  $621.26 \times 10^{-3} \mu\text{m}^2$ . The majority of permeability values are distributed within the range of less than  $50 \times 10^{-3} \mu\text{m}^2$  (Table 1). Therefore, the Cretaceous Qushuibe Formation and Hutubi Formation in the study area are predominantly characterized as low-porosity, low-permeability reservoirs, with a few areas exhibiting moderate-porosity, moderate-permeability, and high-porosity, high-permeability reservoirs (Figure 4).

**4.3. Pore Type Characteristics.** The pore types and structural characteristics of reservoirs directly determine the reservoir's petrophysical properties.<sup>45–47</sup> Through core observation, thin-section analysis, and scanning electron microscopy analysis, statistics indicate that the predominant pore

**Table 1. Statistical Table for Pore Permeability Data of Some Samples in the Target Layer in the Study Area**

| formation        | depth (m) | porosity (%) | permeability ( $10^{-3} \mu\text{m}^2$ ) |
|------------------|-----------|--------------|--|
| K <sub>1</sub> q | 452.57    | 34.51        | 621.26                                   |
| K <sub>1</sub> q | 452.65    | 34.00        | 559.92                                   |
| K <sub>1</sub> q | 453.70    | 31.72        | 579.04                                   |
| K <sub>1</sub> q | 490.06    | 21.41        | 19.38                                    |
| K <sub>1</sub> q | 442.13    | 13.23        | 18.27                                    |
| K <sub>1</sub> q | 453.05    | 33.41        | 159.72                                   |
| K <sub>1</sub> q | 442.56    | 13.92        | 26.01                                    |
| K <sub>1</sub> q | 443.65    | 10.11        | 4.05                                     |
| K <sub>1</sub> q | 444.25    | 9.42         | 2.81                                     |
| K <sub>1</sub> h | 450.13    | 21.61        | 324.85                                   |
| K <sub>1</sub> h | 457.35    | 8.63         | 1.88                                     |
| K <sub>1</sub> h | 458.80    | 11.41        | 3.12                                     |
| K <sub>1</sub> h | 459.75    | 9.62         | 6.23                                     |
| K <sub>1</sub> h | 460.10    | 14.13        | 5.15                                     |
| K <sub>1</sub> h | 460.84    | 13.23        | 12.40                                    |
| K <sub>1</sub> h | 456.30    | 12.92        | 12.74                                    |
| K <sub>1</sub> h | 456.65    | 10.91        | 7.03                                     |
| K <sub>1</sub> h | 450.70    | 16.63        | 14.34                                    |
| K <sub>1</sub> h | 452.30    | 10.91        | 0.90                                     |
| K <sub>1</sub> h | 455.74    | 12.73        | 5.37                                     |

types in the Cretaceous reservoirs of the study area are primary pores, accompanied by the development of secondary pores and a small number of microfractures (Figures 5 and 6). The most predominant pore type is intergranular pores, accounting for over 57% of the total porosity, followed by feldspar dissolution pores, accounting for approximately 28% of the total porosity, and a small portion of residual dissolution pores, accounting for approximately 15% of the total porosity. The pore morphology is predominantly irregular, with a few resembling polygons or triangles, and the pore sizes are generally concentrated in the range of 0.13–0.40 mm. The reservoir sandstone exhibits good connectivity of channels, with the main channel types being neck constriction channels and sheet-like channels, followed by curved sheet channels. Some channels are connected through microfractures, and the sorting is moderate.

**4.4. Sedimentary Facies Characteristics.** The study area exhibits stratigraphic development from the Late Paleozoic to the Cenozoic, with the succession of the Carboniferous, Permian, Triassic, Jurassic, Cretaceous, and Quaternary systems.<sup>16,48–50</sup> The main oil-bearing formations are the

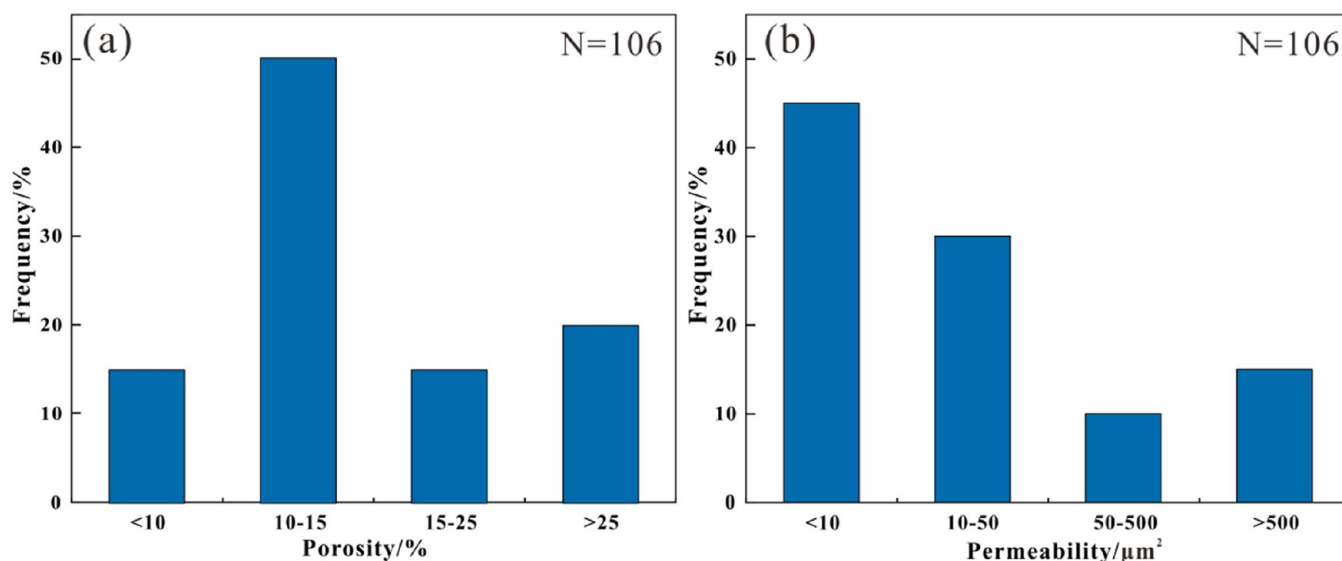


**Figure 4.** Frequency histogram of porosity and permeability distribution in the study area. (a) Porosity distribution frequency; (b) permeability distribution frequency.

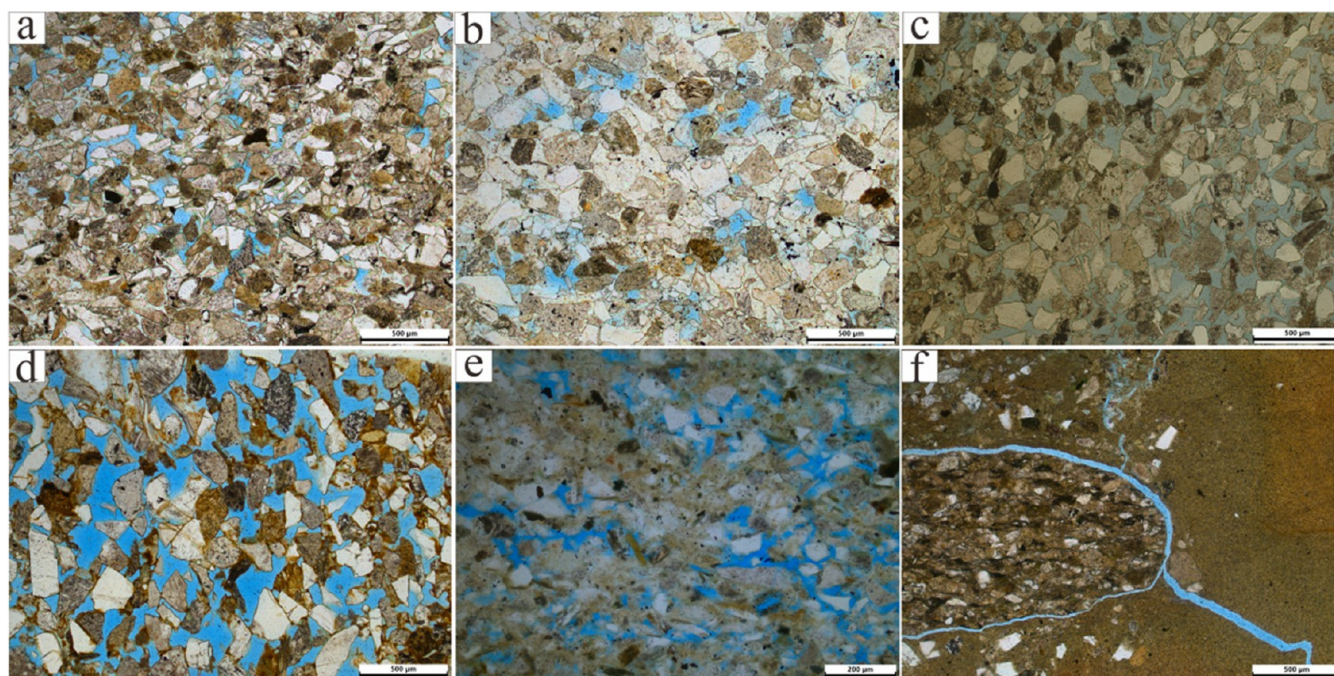


**Figure 5.** Pore characteristics of the  $K_{1q}$  and  $K_{1h}$  in the study area. (a) Hq21-q16, 456.37 m, primary intergranular pore; (b) Hq21-q10, 423.59 m, intergranular pores; (c) Hq23-q22, 423.59 m, primary intergranular pore; (d) Hq23-q50, 218.40 m, particle suspension; (e) Hq23-q48, 135.27 m, dissolution intergranular pore; and (f) Hq23-q42, 88.14 m, dissolution microfracture.

Jurassic and Cretaceous systems, while the focus of this study is on the  $K_{1q}$  and  $K_{1h}$ <sup>19</sup> formations. In this study, based on the sedimentary, cyclical, well logging, and seismic response characteristics, the  $K_{1q}$  formation is subdivided into the  $K_{1q_2}$  and  $K_{1q_3}$  formations, while the  $K_{1h}$  formation is divided into  $K_{1h_1}$ ,  $K_{1h_2}$ , and  $K_{1h_3}$  formations. The total thickness of the strata is approximately 276–1228m. The predominant lithologies present in the study area include siltstone, fine sandstone, conglomerate, and a significant amount of mudstone (Figure 7).

Based on the observation of core samples from shallow wells, mudstone development is observed in both the  $K_{1q}$  and  $K_{1h}$  formations in the study area. According to the core photos and

in conjunction with the lithofacies characteristics of individual wells, the mudstone is predominantly gray in color, with some wells also exhibiting gray green and reddish brown mudstone. Due to the occurrence of stratigraphic overlap in the Cretaceous system of the study area, coarse-grained conglomerate sediment supplied by the provenance has continuously advanced and overlaid under the influence of hydraulic dynamics and tectonic forces. This has resulted in the distribution of conglomerate sediment in both the  $K_{1q}$  and  $K_{1h}$  formations. Combined with the continuous progression of sequence boundaries from the  $K_{1q}$  formation, there is an occurrence of conglomerate distribution at the lowermost part of the Cretaceous stratigraphy in the study area, displaying an

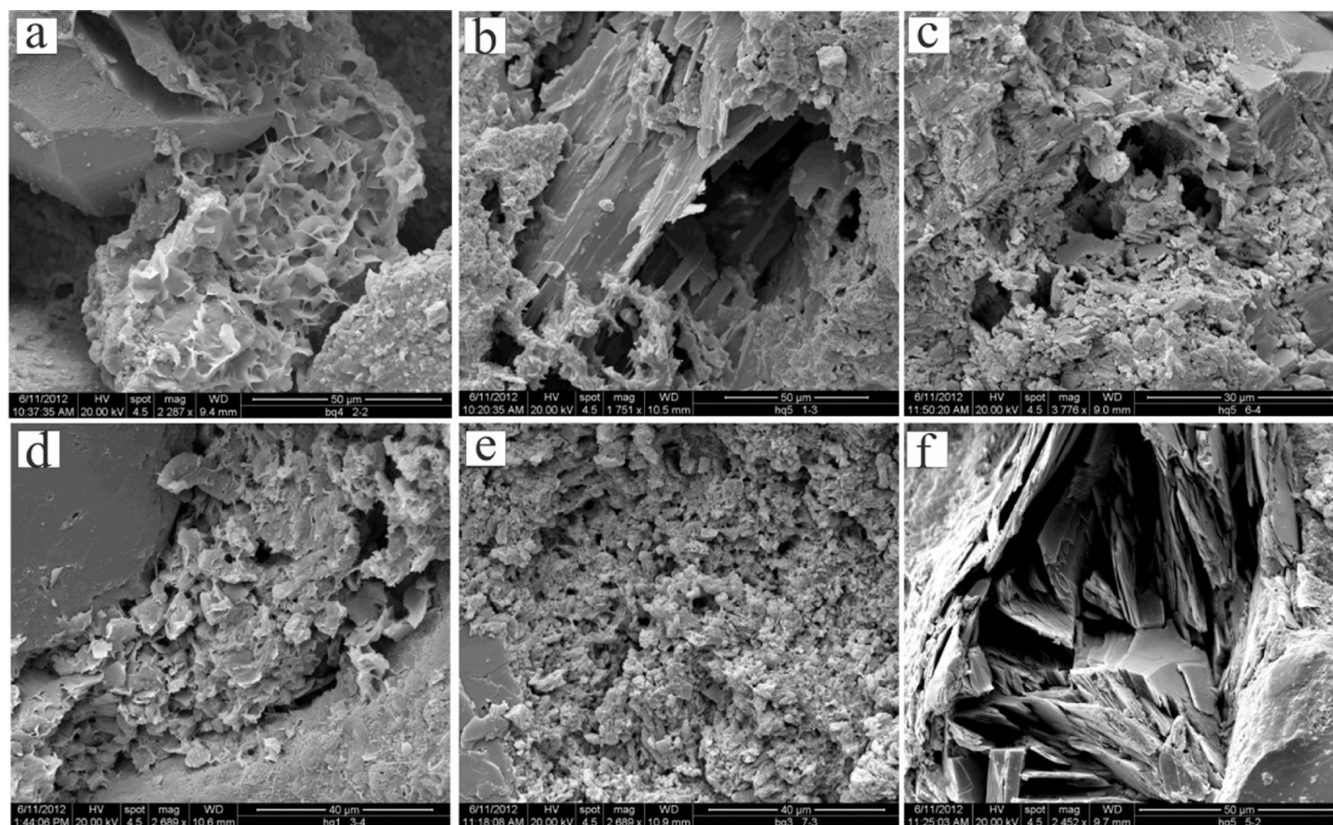


**Figure 6.** Scanning electron microscopic characteristics of  $K_{1q}$  and  $K_{1h}$  in the study area. (a) Bq4, 2287 times, 384.2 m, quartz secondary enlarged pores; (b) Bq2, 2564 times, 242.7 m, feldspar dissolution pore; (c) Bq2, 600 times, 242.7 m, rock debris dissolution pore; (d) Hq21, 2689 times, 301.5 m, quartz secondary enlarged pores; (e) Hq23-q6, 2564 times, 160.12 m, rock debris dissolution pore; and (f) Hq23-q6, 1918 times, 182.1 m, mictization secondary pore.

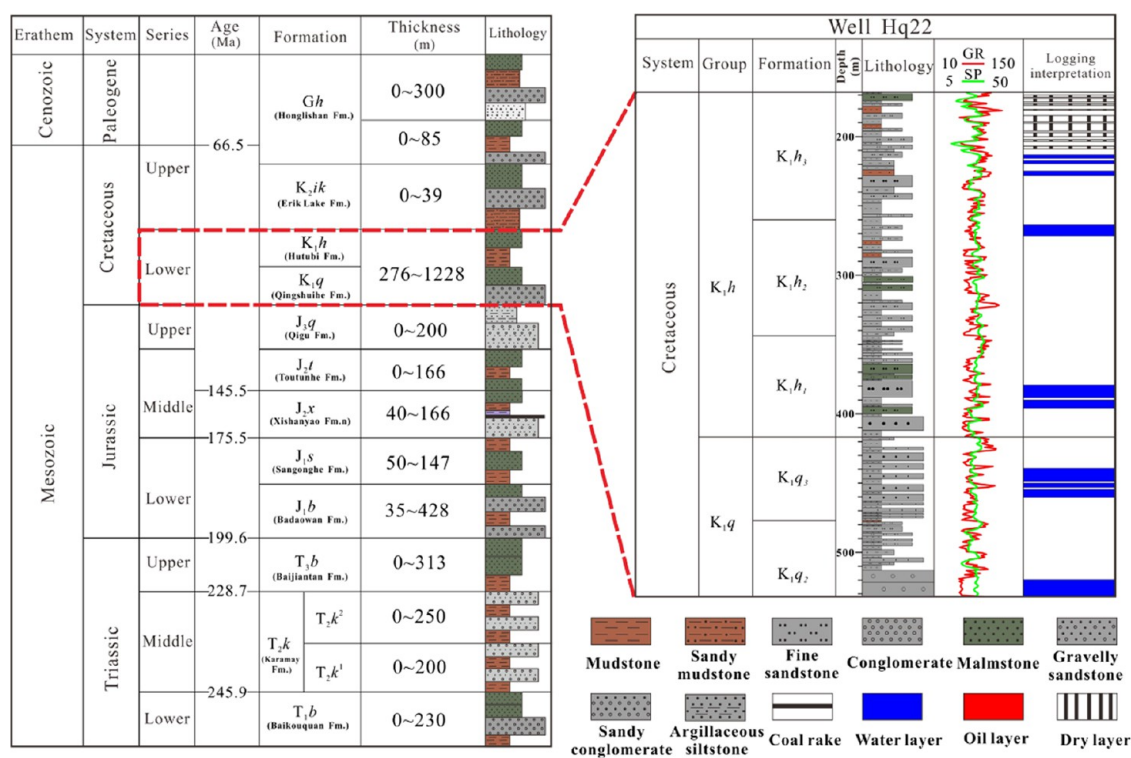


**Figure 7.** Cretaceous stratigraphic development<sup>19</sup> and interpretation of single Hq22 in the Cretaceous system in the study area.

| System  | Cretaceous                            |  |  |                                |                                    |                      |              |
|---|---------------------------------------|--|--|--------------------------------|------------------------------------|----------------------|--------------|
| Group   | K <sub>1</sub> q (Qingshuihe Fm.)     |  |  | K <sub>1</sub> h (Hutubi Fm.)  |                                    |                      |              |
| Formation   | K <sub>1</sub> q <sub>2</sub>         | K <sub>1</sub> q <sub>3</sub>                      | K <sub>1</sub> h <sub>1</sub>            | K <sub>1</sub> h <sub>2</sub>  | K <sub>1</sub> h <sub>3</sub>      |                      |              |
| Sedimentary facies                                | Lacustrine                            | Fan delta-Lacustrine                               |  |                                |                                    |                      |              |
| Subfacies   | Fan delta plain                       | Fan delta plain-Fan delta front-Shore-shallow lake |  |                                |                                    |                      |              |
| Core photos                                       |                                       |  |  |                                |                                    |                      |              |
|   | Hq21-q6, 420.81m<br>Siltstone         | Hq21-q9, 452.13m<br>Argillaceous siltstone         | Hq23-q1, 329.92m<br>Silty fine sandstone | Bq3, 246.18m<br>Fine sandstone | Hq23-q8, 157.65m<br>Sandy mudstone |                      |              |
|   | G.R<br>API<br>61-130                  | G.R<br>API<br>52-112                               | G.R<br>API<br>61-130                     | G.R<br>API<br>1-100            | G.R<br>API<br>50-110               |                      |              |
|   | Depth (m)<br>410<br>415<br>420<br>425 | Depth (m)<br>450<br>454                            | Depth (m)<br>335                         | Depth (m)<br>246<br>250<br>254 | Depth (m)<br>150                   |                      |              |
|   | Lithology                             | Lithology  | Lithology                                | Lithology                      | Lithology                          |                      |              |
| Electric characteristics and Sedimentary sequence |                                       |  |  |                                |                                    |                      |              |
|   | Siltstone                             | Fine sandstone                                     | Mudstone                                 | Parallel bedding               | Oblique bedding                    | Trough cross-bedding | Boulder clay |

Figure 8. Typical sedimentary facies characteristics of the K<sub>1</sub>q and K<sub>1</sub>h formations in the study area.

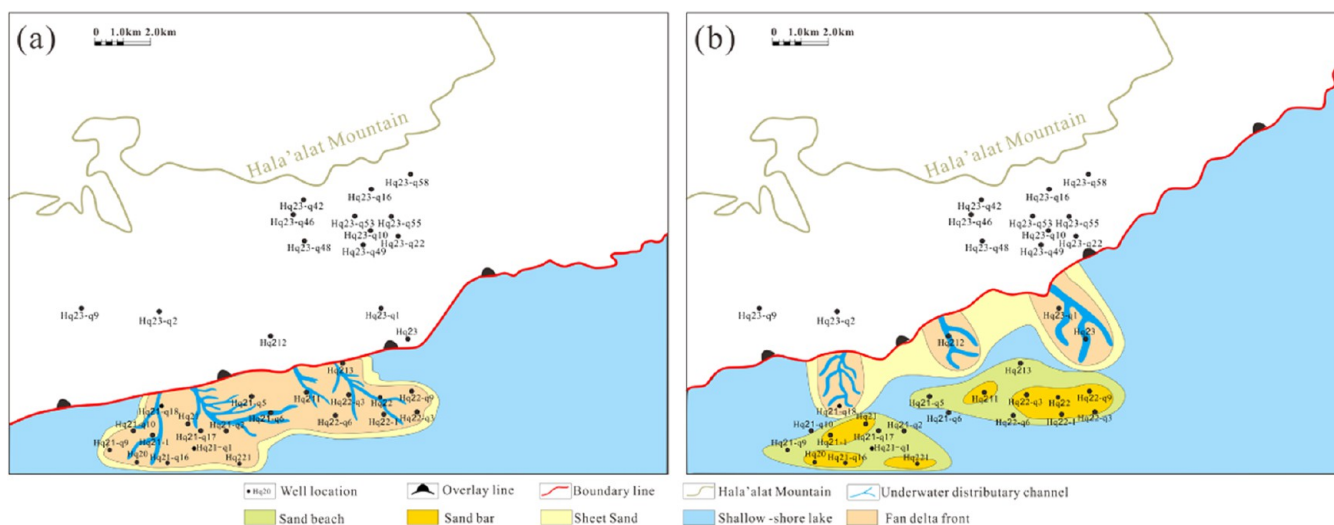


Figure 9. Distribution characteristics of typical sedimentary facies of Qingshuihe formation of Cretaceous in the study area. (a) K<sub>1</sub>q<sub>2</sub> formation sedimentary facies plan; (b) K<sub>1</sub>q<sub>3</sub> formation sedimentary facies plan.

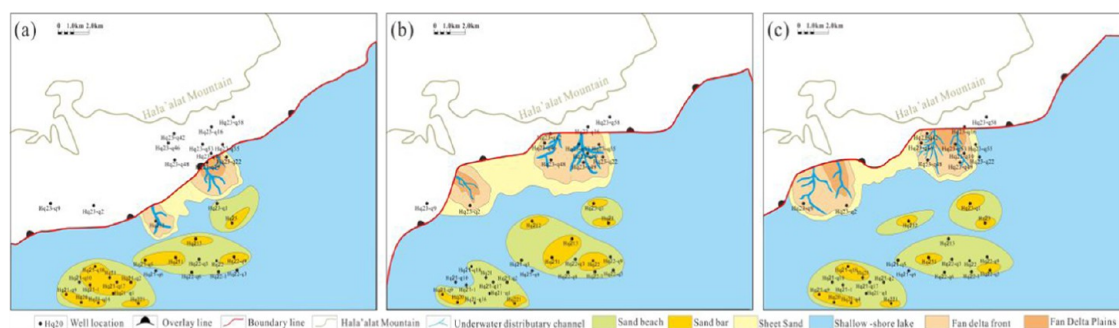


Figure 10. Distribution characteristics of typical sedimentary facies of Hutubi formation of Cretaceous in the study area. (a) K<sub>1</sub>h<sub>1</sub> formation sedimentary facies plan; (b) K<sub>1</sub>h<sub>2</sub> formation sedimentary facies plan; and (c) K<sub>1</sub>h<sub>3</sub> formation sedimentary facies plan.

overall gray color (Figure 8). It is concluded that the coarse-grained deposits of fan delta facies were mainly developed in the early Cretaceous, and the main sedimentary subfacies were fan delta front subfacies (Figure 9). Multiple channels could be identified, and the superposition of channels made the sand

bodies thicker and distributed in dendritic shape from northwest to southeast, and the sand distributed in a wide range. The upward grain size becomes finer, and the sedimentary facies transition to beach-bar facies deposition of shore-shallow lake. In this process, the branches of the river



tend to disperse, thus forming multiple branch channels. As the water surface rises, the environment of the shore-shallow lake expands continuously, and the sediments begin to deposit in the direction of water depth, resulting in the emergence of large-scale beach-bar deposition (Figure 10).

## 5. DISCUSSIONS

**5.1. Single-Factor Evaluation of Reservoirs.** To enhance the accuracy of reservoir evaluation, this study employs a multifactor comprehensive evaluation method to achieve a more effective assessment of the Cretaceous reservoirs in the study area. The evaluation method involves assessing three key macroscopic factors: the lithology coefficient, storage coefficient, and flow zone index (Table 2). Based on these evaluations and incorporating microscale

**Table 2. Statistical Table of Multiple Single-Factor Comprehensive Evaluation Results for Some Samples in the Study Area**

| formation | depth (m) | formation factor ( $K_h$ ) | storage coefficient ( $\Phi_h$ ) | flow zone index (FZI) |
|-----------|-----------|----------------------------|----------------------------------|-----------------------|
| $K_{1q}$  | 452.57    | 77.46                      | 0.04                             | 1.26                  |
| $K_{1q}$  | 452.65    | 65.19                      | 0.08                             | 1.22                  |
| $K_{1q}$  | 453.7     | 54.66                      | 0.71                             | 1.26                  |
| $K_{1q}$  | 490.06    | 25.68                      | 0.06                             | 0.04                  |
| $K_{1q}$  | 442.13    | 125.84                     | 0.02                             | 0.14                  |
| $K_{1q}$  | 453.05    | 58.59                      | 0.32                             | 0.68                  |
| $K_{1q}$  | 442.56    | 84.78                      | 0.1                              | 0.27                  |
| $K_{1h}$  | 365.58    | 125.4                      | 0.632                            | 1.66                  |
| $K_{1h}$  | 311.03    | 329.55                     | 0.31                             | 2.1                   |
| $K_{1h}$  | 311.68    | 190.15                     | 0.55                             | 2.26                  |

parameters obtained through experimental analysis, a classification standard for the reservoir is established. In this experiment, 87 core samples were selected for testing, and a comprehensive evaluation of multiple factors was conducted on the reservoir quality in the study area, resulting in the classification of the Cretaceous reservoirs in the study area into three categories: Class A (good reservoir), Class B (moderate reservoir), and Class C (poor reservoir).

**5.1.1. Evaluation Results of the Formation Coefficient.** By applying the I formation coefficient ( $K_h$ ) evaluation method, an assessment of the quality of the Cretaceous reservoirs in the study area was conducted. The results indicate that the lithology coefficient for most of the  $K_{1q}$  formation and the  $K_{1h}$  formation reservoirs falls within the range of 15–70, followed by a smaller portion exceeding 70, and a minority with values below 15 (Figure 11a,b). Based on the cumulative frequency curves of the lithology coefficient, the reservoirs of the  $K_{1q}$  and  $K_{1h}$  formations in the study area were classified. The classification was determined by the lithology coefficients corresponding to the 75 and 25% cumulative frequencies, resulting in the subdivision of the  $K_{1q}$  and  $K_{1h}$  formation reservoirs into three categories. Class A reservoirs have a formation coefficient greater than 70, indicating excellent reservoir quality. Reservoirs with a formation coefficient ranging from 15 to 70 are considered to have good reservoir quality. Reservoirs with a formation coefficient of less than 15 are classified as poor reservoirs. The vertical distribution characteristics of the evaluation results of Hq22–1 ~ Hq212 have been drawn in the study area (Figure 12).

**5.1.2. Evaluation Results of the Storage Coefficient.** By employing the storage coefficient evaluation method, the quality assessment of the Cretaceous reservoirs in the study area was conducted. The storage coefficient of the  $K_{1q}$  formation in the study area is predominantly distributed within the range of less than 0.5, indicating a good sorting degree. The remaining portion is distributed within the range 0.5–1.4, indicating a poor sorting degree (Figure 13a). Similarly, a statistical analysis was conducted on the storage coefficient of the  $K_{1h}$  formation in the study area. It was found that the majority of the storage coefficients are distributed within the range of less than 0.5, indicating a poor sorting degree. The remaining portion is distributed within the range of 0.5–1.4, indicating a moderate sorting degree (Figure 13b). Based on the cumulative frequency curve of the storage coefficient, the reservoirs of the  $K_{1q}$  and  $K_{1h}$  formations in the study area were classified. The storage coefficients corresponding to the cumulative frequencies at 75 and 25% were used to divide the  $K_{1q}$  and  $K_{1h}$  formation reservoirs into three categories. A-

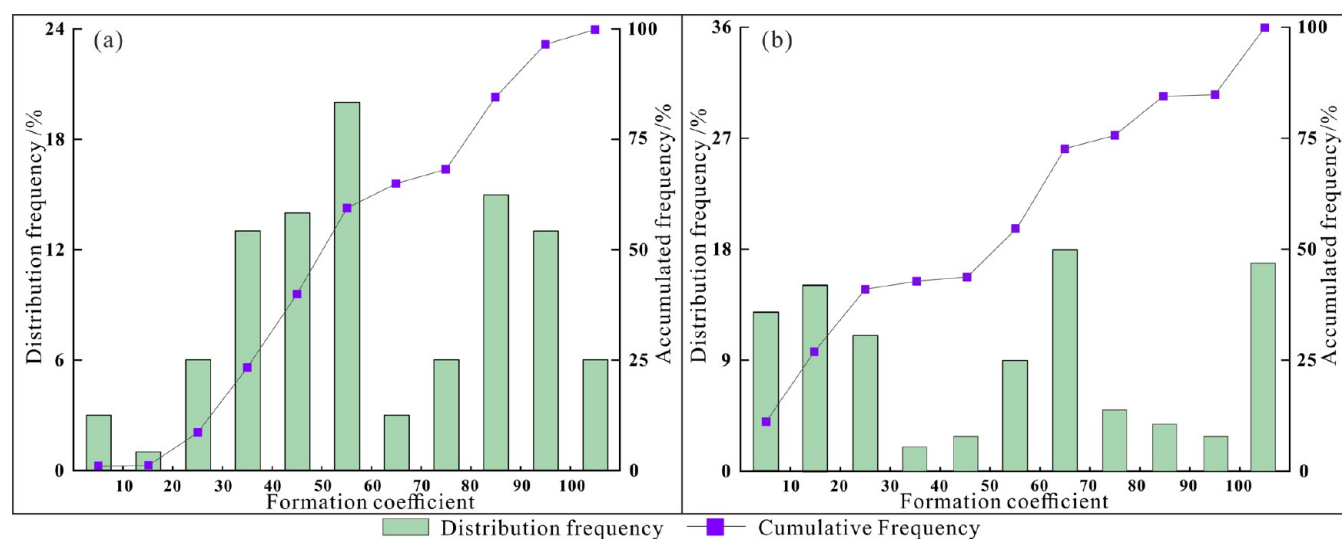


**Figure 11.** Presents the histogram of the distribution of lithology coefficients for the Cretaceous formations in the study area. (a)  $K_{1q}$  formation; (b)  $K_{1h}$  formation.

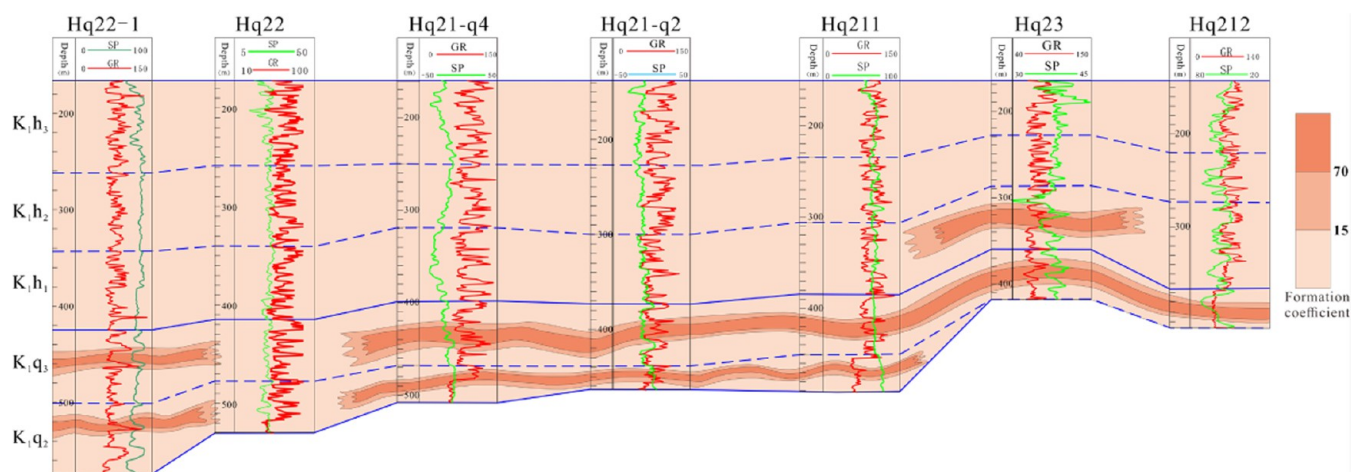


**Figure 12.** Vertical distribution characteristics of the evaluation results of formation coefficients for Hq22-1 ~ Hq212 locations in the study area.

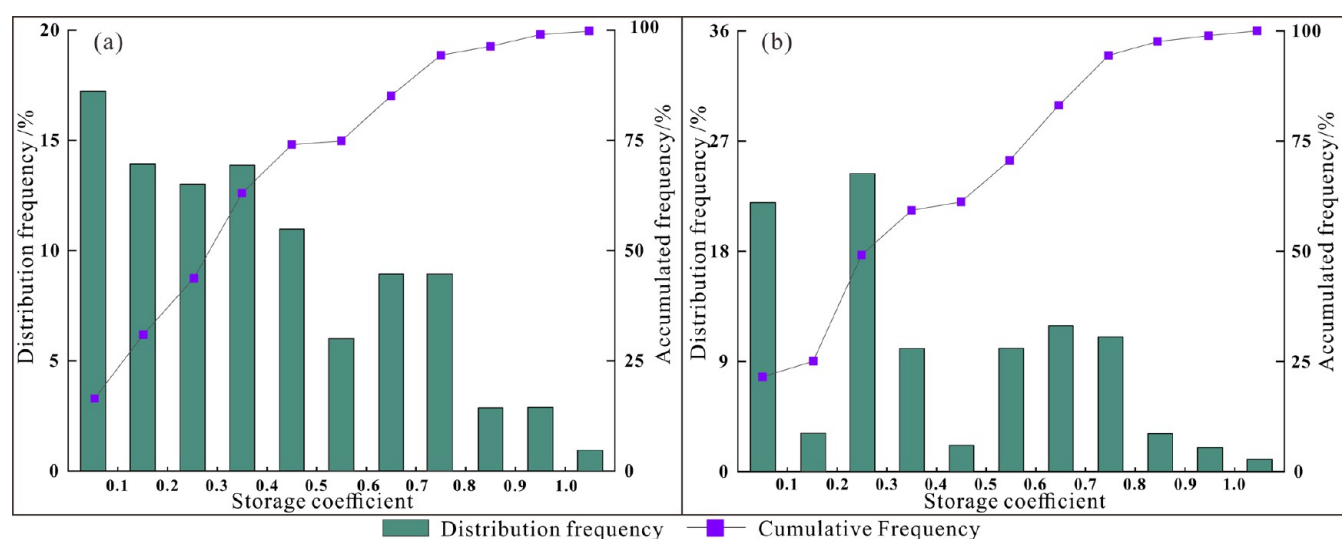


**Figure 13.** Histogram of storage coefficient distribution in the cretaceous system in the study area. (a)  $K_{1q}$  formation; (b)  $K_{1h}$  formation.

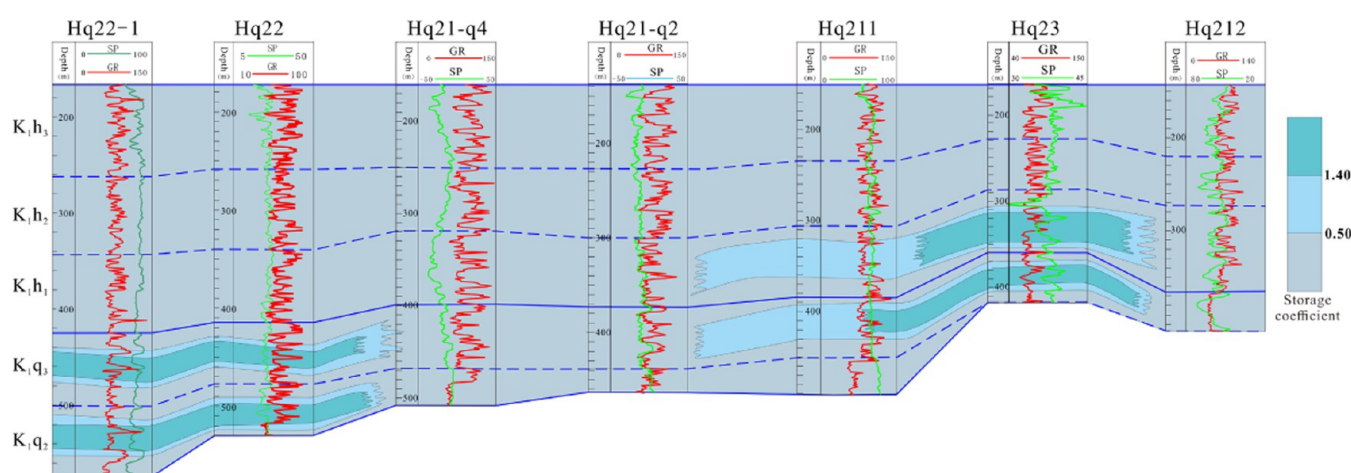


**Figure 14.** Vertical distribution characteristics of the evaluation results of storage coefficients for Hq22-1 ~ Hq212 locations in the study area.

class reservoirs, with storage coefficients greater than 1.4, are considered as good reservoirs. Reservoirs with storage coefficients ranging from 0.5 to 1.4 are classified as relatively good reservoirs, while reservoirs with storage coefficients less than 0.5 are considered as relatively poor reservoirs. The

vertical distribution characteristics of the evaluation results of Hq22-1 ~ Hq212 have been drawn in the study area (Figure 14).

**5.1.3. Evaluation Results of the Flow Units.** Based on the stratigraphic division, this study primarily investigates the

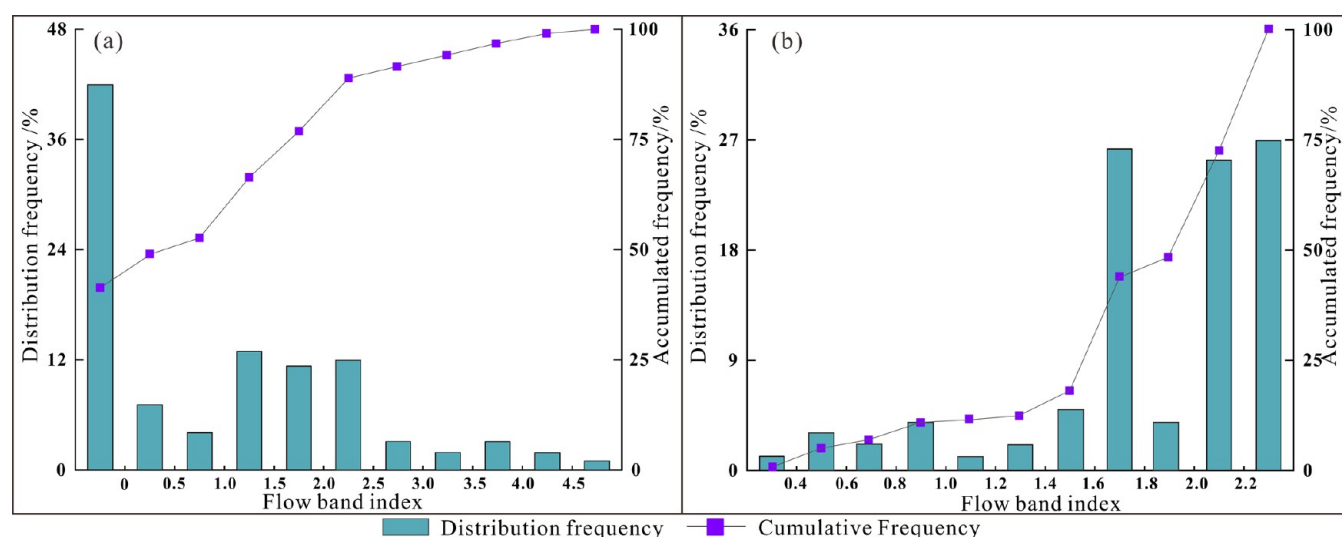


**Figure 15.** Histogram of the index distribution of the Cretaceous flow zone in the study area. (a)  $K_{1q}$  formation; (b)  $K_{1h}$  formation.

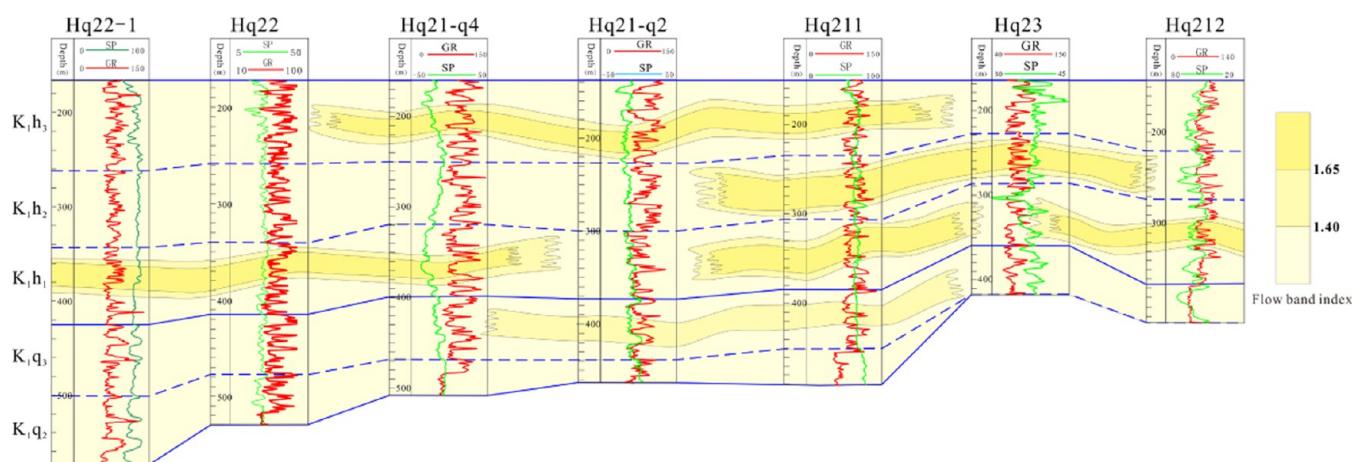


**Figure 16.** Vertical distribution characteristics of flow unit index evaluation results for Hq22-1 ~ Hq212 locations in the study area.

spatial distribution pattern of flow units in the reservoirs of the study area within the Cretaceous system. The majority of the flow zone index values within the study area's  $K_{1q}$  formation are below 1.4, with a very small portion distributed between 1.40 and 1.65, while the remaining portion shows a relatively uniform distribution above 1.65 (Figure 15a). Similarly, the flow zone index of the  $K_{1h}$  formation reservoirs shows that the majority of values are above 1.65, with a small portion distributed between 1.40 and 1.65, while the remaining portion exhibits a relatively uniform distribution below 1.40 (Figure 15b). Based on the cumulative frequency curve of the flow zone index, a study was conducted on the flow units of the  $K_{1q}$  and  $K_{1h}$  formation reservoirs in the study area. According to the flow zone index corresponding to the 75 and 25% percentiles of the cumulative frequency, the reservoirs of the  $K_{1q}$  and  $K_{1h}$  formations in the study area were classified into three categories. A-class reservoirs have a flow zone index (FZI) greater than 1.65, indicating good reservoir quality. Reservoirs with an FZI ranging from 1.40 to 1.65 are classified as moderately good reservoirs, while those with an FZI less than 1.4 are considered poor reservoirs. The vertical distribution characteristics of the evaluation results of Hq22-1 ~ Hq212 have been drawn in the study area (Figure 16).

Based on the three single-factor evaluation results of the reservoirs in the  $K_{1q}$  and  $K_{1h}$  formations in the study area, the following reservoir evaluation classification criteria are summarized for the study area (Table 3).

**Table 3. Classification Criteria for Single-Factor Evaluation of Reservoirs in the Study Area**

| reservoir type | formation coefficient | storage coefficient | flow zone index | reservoir evaluation |
|----------------|-----------------------|---------------------|-----------------|----------------------|
| A              | >70                   | >1.4                | >1.65           | good                 |
| B              | 15–70                 | 0.5–1.4             | 1.40–1.65       | medium               |
| C              | <15                   | <0.5                | <1.40           | poor                 |

**5.2. Integrated Reservoir Evaluation Results.** Based on the above classification criteria and evaluation methods, as well as the reservoir lithological characteristics, reservoir petrophysical properties, and pore structure characteristics described earlier, classification and evaluation maps of the reservoirs in the study area, including the  $K_{1q}$  and  $K_{1h}$  formations, were generated. The distribution of the four reservoir categories is controlled by the sedimentary facies. Class I and Class II reservoirs are generally found in braid-like channels with thick sand bodies and good continuity. Class III reservoirs are

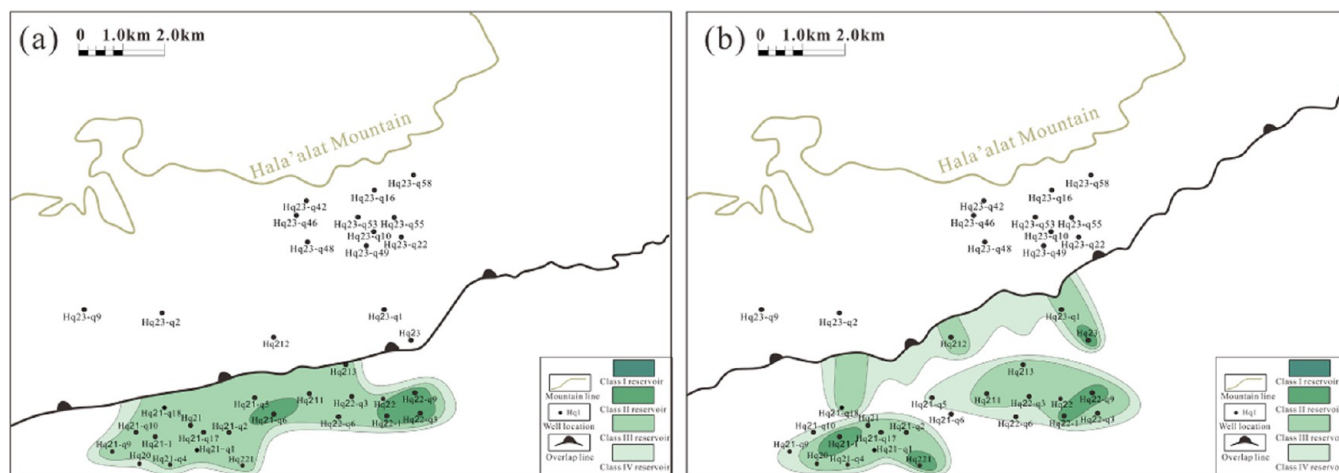


**Figure 17.** Comprehensive evaluation of reservoir classification of the  $K_1q$  formation in the study area. (a)  $K_1q_2$  formation; (b)  $K_1q_3$  formation.

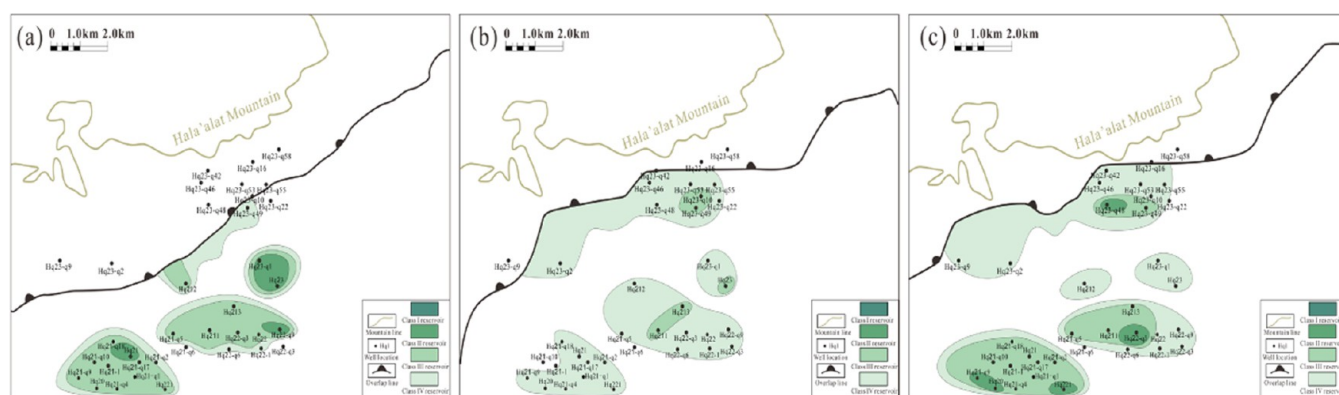


**Figure 18.** Comprehensive evaluation of reservoir classification of the  $K_1h$  formation in the study area. (a)  $K_1h_1$  formation; (b)  $K_1h_2$  formation; and (c)  $K_1h_3$  formation.

typically distributed in sand bars, while Class IV reservoirs are located between subaqueous distributary channels on the flanks of channels with thinner sand sedimentation.

The study area of the  $K_1q$  primarily comprises two segments, namely,  $K_1q_2$  and  $K_1q_3$  formations. The  $K_1q_2$  formation is characterized by the development of fan delta depositional facies, whereas the  $K_1q_3$  formation primarily exhibits fan delta and nearshore lacustrine barrier bar facies. The  $K_1h$  formation is characterized by the development of three segments, namely,  $K_1h_1$ ,  $K_1h_2$ , and  $K_1h_3$  formations, all of which exhibit fan delta and nearshore lacustrine barrier bar facies.

By evaluating the reservoir quality in the study area through three key single factors: formation coefficient, storage coefficient, and flow zone index, combined with various experimental analysis data, thin-section identification results, and previous research findings, a comprehensive reservoir quality evaluation chart was generated. From Figure 17(a), it can be observed that in the  $K_1q_2$  formation, there is no distribution of Class I reservoirs. Class II reservoirs are distributed in clustered patterns within the Hq21-q6 well area, Hq22-1 well area, Hq22-q3 well area, and Hq22-q9 well area. Class III and Class IV reservoirs exhibit continuous distribution with a wide distribution of effective areas. From Figure 17(b), it can be observed that in the  $K_1q_3$  formation, Class II reservoirs are distributed in small clustered patterns dispersed within different blocks. They are distributed in the Hq21-1 well area, Hq221 well area, Hq22-1 well area,

Hq22-2 well area, Hq22-q9 well area, and Hq23 well area. The remaining effective reservoir sections are predominantly Class III and Class IV reservoirs.

Similarly, from Figure 18(a), it can be observed that in the  $K_1h_1$  formation, Class II reservoirs are dispersedly distributed in the Hq21 well area, Hq22-q9 well area, Hq23 well area, and Hq23-q1 well area. The remaining effective reservoir sections are predominantly distributed as Class III and Class IV reservoirs. From Figure 18(b), it can be observed that in the  $K_1h_2$  formation, the reservoir quality is poor, with no Class I or Class II reservoirs present. Class III reservoirs exhibit various shapes and are dispersedly distributed in different exploration areas, including the Hq21-q9 well area, Hq21 well area, Hq221 well area, Hq21-q2 well area, Hq21-q12 well area, Hq22-q5 well area, Hq23 well area, Hq23-q49 well area, and Hq23-q10 well area. The remaining portions consist of Class IV reservoirs. From Figure 18(c), it can be observed that in the  $K_1h_3$  formation, Class II reservoirs are dispersedly distributed in different exploration areas, including the Hq21-q9 well area, Hq20 well area, Hq221 well area, Hq22-q1 well area, Hq22-3 well area, Hq22-q10 well area, Hq23-q1 well area, and Hq23-q48 well area. The remaining portions consist of Class III and Class IV reservoirs.

### 5.3. Verification of Reservoir Classification Results.

The delineation of varying reservoir quality is primarily demonstrated through differences in the production capacity. As such, this investigation employed Poisson's ratio parameters

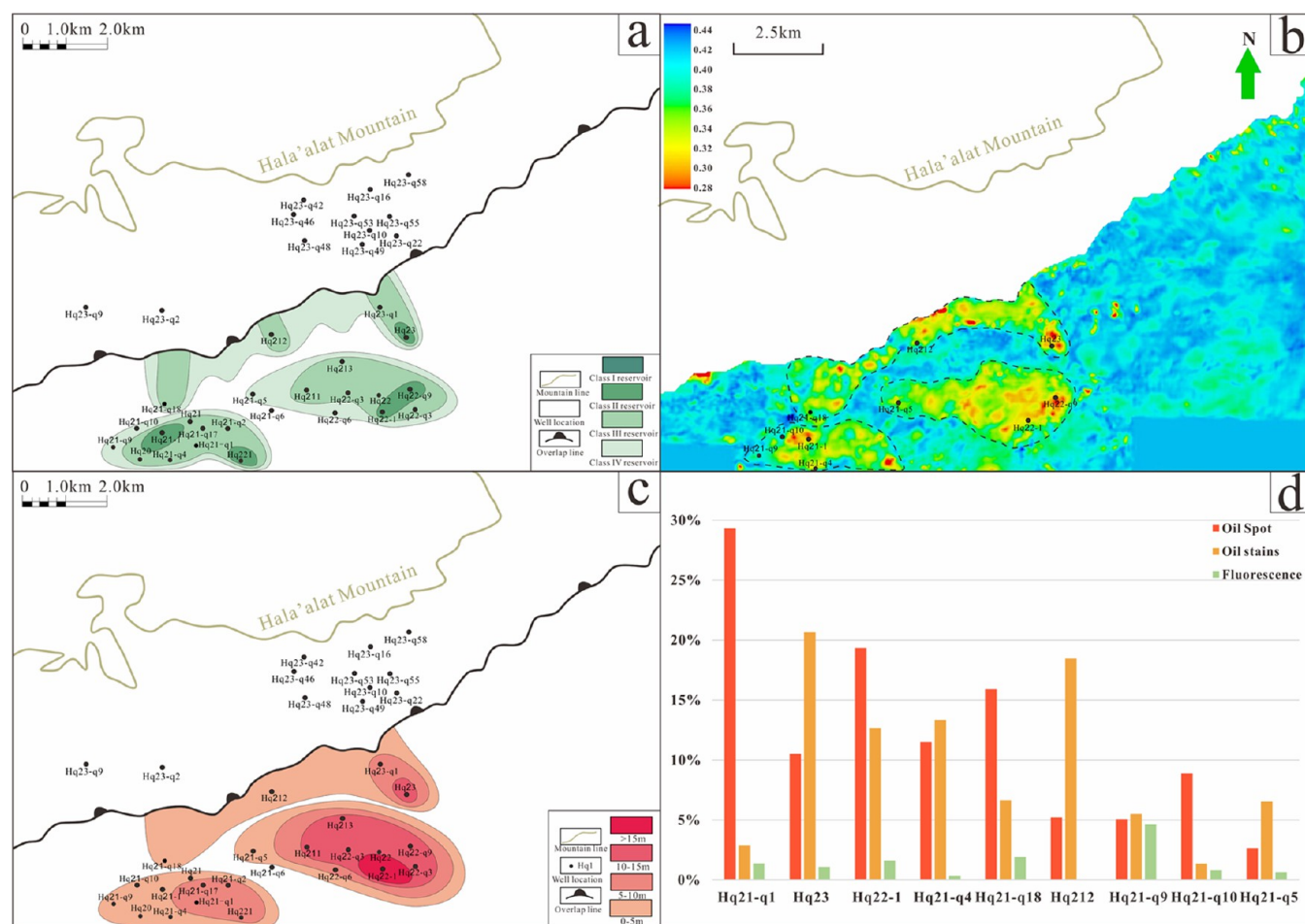


**Figure 19.** Verification diagram of reservoir classification evaluation results. (a)  $K_{1q3}$  formation reservoir classification evaluation map; (b)  $K_{1q3}$  formation reservoir Poisson's ratio parameter plan; (c)  $K_{1q3}$  formation oil layer thickness plan; and (d)  $K_{1q3}$  formation Hq21-q1 ~ Hq21-q5 histogram of oil type differences.

to accurately reflect reservoir evaluation outcomes, which were subsequently validated by assessing variations in oil layer thickness distribution and content. Using wells Hq21-q1 ~ Hq21-q5 as examples, we have verified the reservoir quality classification results of the  $K_{1q3}$  formations in the study area. The inversion results of the Poisson's ratio parameters for this member have been obtained (Figure 19b). The yellow and red areas in the figure represent zones of relatively low Poisson's ratio, and the lower the value, the better the oil content. Wells Hq23, Hq21-1, Hq22-1, and Hq221 in the study area are situated within the low Poisson's ratio zones, indicating relatively good oil-bearing properties. Based on the oil layer thickness distribution and differences in oil-bearing types at different well locations, we can conclude that the Hq21-1, Hq23, and Hq22-1 well areas possess favorable oil-bearing properties (Figure 19c,d). In summary, the reservoir quality classification evaluation results (Figure 19a) align closely with actual geological knowledge. These evaluations adeptly classify reservoir types, rendering positive prospects for predicting advantageous sandstone reservoirs and offering beneficial insights into sandstone reservoir quality evaluations in other areas.

## 6. CONCLUSIONS

(1) The single-factor reservoir evaluation method has shown good application effectiveness in rational reservoir

delineation and improving the accuracy of permeability interpretation. Compared to conventional reservoir evaluation methods, the single-factor evaluation method provides a more precise and effective approach to reservoir quality classification, based on the classification criteria established according to the principles of different single-factor evaluation methods.

- (2) Research has shown that relying solely on a single-factor method to evaluate reservoir quality has limitations. In this study, we primarily utilized the results of three single-factor evaluations: formation factor ( $K_h$ ), storage coefficient ( $\Phi_h$ ), and flow zone indicator (FZI). These evaluations were further combined with experimental data such as core observation, thin-section analysis, porosity-permeability analysis, and scanning electron microscopy. The integrated study focused on the spatial distribution patterns of A-class reservoirs based on the individual evaluations. Finally, a comprehensive set of reservoir quality classification criteria was developed.
- (3) By applying this method to the classification of reservoir quality in the study area, the conclusions drawn are consistent with the actual field development, validating the accuracy and effectiveness of the method. It demonstrates the integration between reservoir storage capacity, production capacity, petrophysical characteristics, and the micropore structure of the reservoir. It

also aligns well with log interpretation and reservoir properties, providing a solid foundation for the integration of reservoir geology and oil and gas storage and transportation engineering.

## AUTHOR INFORMATION

### Corresponding Author

**Xiao Hu** – School of Natural Resources, Faculty of Geographical Science, Beijing Normal University, Beijing 100875, China; [orcid.org/0000-0002-5971-701X](https://orcid.org/0000-0002-5971-701X); Email: [huxiao0611@mail.bnu.edu.cn](mailto:huxiao0611@mail.bnu.edu.cn)

### Authors

**Qiongyao Pu** – College of Earth Science and Engineering, Shandong University of Science and Technology, Qingdao 266590, China

**Jun Xie** – College of Earth Science and Engineering, Shandong University of Science and Technology, Qingdao 266590, China; [orcid.org/0000-0001-7300-1176](https://orcid.org/0000-0001-7300-1176)

**XinShuai Li** – College of Earth Science and Engineering, Shandong University of Science and Technology, Qingdao 266590, China

**YuanPei Zhang** – College of Earth Science and Engineering, Shandong University of Science and Technology, Qingdao 266590, China

**Xiaofan Hao** – College of Earth Science and Engineering, Shandong University of Science and Technology, Qingdao 266590, China

**Fengrui Zhang** – Oil and Gas Engineering Research Institute of PetroChina Jilin Oilfield Company, Changchun 130062, China

**Zhengquan Zhao** – The fifth oil production plant of PetroChina Huabei Oilfield Company, Shijiazhuang 052360, China

**Jianfeng Cao** – PetroChina Bohai Drilling Fourth Drilling Engineering Branch, Hejian 062552, China

**Yan Li** – College of Earth Science and Engineering, Shandong University of Science and Technology, Qingdao 266590, China

**Renjie Gao** – College of Earth Science and Engineering, Shandong University of Science and Technology, Qingdao 266590, China

Complete contact information is available at:

<https://pubs.acs.org/10.1021/acsomega.3c04449>

### Author Contributions

Q.P.: conceptualization, methodology, validation, formal analysis, writing—original draft, and writing—review and editing. J.X.: conceptualization, formal analysis, resources, writing—review and editing, and funding acquisition. X.L.: methodology, software, validation, and visualization. Y.Z.: methodology, investigation, and visualization. X.H.: conceptualization, methodology, validation, formal analysis, writing—original draft, and writing—review and editing. X.H.: validation, investigation, and data curation. F.Z.: validation, formal analysis, and supervision. Z.Z.: formal analysis, investigation, visualization, and supervision. J.C.: methodology, resources, and data curation. Y.L.: validation, investigation, and data curation. R.G.: software, validation, and data curation.

### Notes

The authors declare no competing financial interest.

## ACKNOWLEDGMENTS

This work was supported by the Natural Science Foundation of Shandong Province: the mechanism of gas water mutual drive in the process of strong injection and strong production of carbonate underground gas storage [No. ZR2022MD033].

## REFERENCES

- (1) Gao, X. L. Reservoir characteristics and classification evaluation of the third member of the Dongying Formation in the Sanqu area of Shengtuo Oilfield Fault-block Oil Gas Field 2011; Vol. 18 02, pp 195–198.
- (2) Zhao, J. F.; Chen, X. H.; Zhang, Q. Application of grey correlation analysis in reservoir evaluation *Adv. Explor. Geophys.* 2003, 04, pp 282–286.
- (3) Loucks, R. G.; Peng, S. Matrix reservoir quality of the Upper Cretaceous Austin Chalk Group and evaluation of reservoir-quality analysis methods; northern onshore Gulf of Mexico, U.S.A. *Mar. Pet. Geol.* 2021, 134, No. 105323.
- (4) Liu, J. J.; Liu, J. C. An intelligent approach for reservoir quality evaluation in tight sandstone reservoir using gradient boosting decision tree algorithm - A case study of the Yanchang Formation, mid-eastern Ordos Basin, China. *Mar. Pet. Geol.* 2021, 126, No. 104939.
- (5) Jiang, D. L.; Chen, H.; Xing, J. P.; Shang, L.; Wang, Q. H.; Sun, Y. C.; Zhao, Y.; Cui, J.; Lan, D. C. A novel method of quantitative evaluation and comprehensive classification of low permeability-tight oil reservoirs: A case study of Jidong Oilfield, China. *Pet. Sci.* 2022, 19 (4), 1527–1541.
- (6) Pan, B. H.; Wang, X. R.; Guo, Y. H.; Zhang, L. H.; A, R. H.; Zhang, N. Y.; Zhang, P. J.; Li, Y. Study on reservoir characteristics and evaluation methods of altered igneous reservoirs in Songliao Basin, China. *J. Pet. Sci. Eng.* 2022, 212, No. 110266.
- (7) Wu, B. H.; Xie, R. H.; Xiao, L. Z.; Guo, J. F.; Jin, G. W.; Fu, J. W. Integrated classification method of tight sandstone reservoir based on principal component analysis - simulated annealing genetic algorithm - fuzzy cluster means *Pet. Sci.* 2023, DOI: [10.1016/j.petsci.2023.04.014](https://doi.org/10.1016/j.petsci.2023.04.014).
- (8) Ren, Y.; Wei, W.; Zhu, P.; Zhang, X. M.; Chen, K. Y.; Liu, Y. S. Characteristics, classification and KNN-based evaluation of paleokarst carbonate reservoirs: A case study of Feixianguan Formation in northeastern Sichuan Basin, China. *Energy Geosci.* 2023, 4 (3), No. 100156.
- (9) Shalaby, M. R.; Thota, S. T.; Norsahminan, D. N. P.; Kamalrulzaman, K. N.; Matter, W. S.; Al-Awah, H. Reservoir quality evaluation using petrophysical, well-log analysis and petrographical description: A case study from the Carboniferous-Permian Kulshill group formations, southern Bonaparte Basin, Australia. *Geoenergy Sci. Eng.* 2023, 226, No. 211738.
- (10) Sun, H. Z.; Liu, J. Q. Research on comprehensive quantitative evaluation method of reservoirs *Research on Comprehensive Quantitative Evaluation Method of Reservoirs* 2004, 06, pp 8–10 + 89.
- (11) Li, S. B. *Comprehensive geological evaluation and adjustment management study of the Wangji complex fault-block reservoir development*. Doctor, Southwest Petroleum University 2010.
- (12) Yang, S. S.; Zhao, Y. G.; Liu, X. J.; Chen, Y.; Yang, Y. Reservoir characteristics and reservoir quality evaluation of Chang-2 in southeastern Jingbian area *Block Oil Gas Fields* 2014; Vol. 21 02, pp 157–160 + 180.
- (13) Li, C. Y.; Chen, W. H.; Fu, Y. M.; Tony Reservoir classification evaluation using the flow unit index *Sino-Global Energy* 2012; Vol. 17 10, pp 40–43.
- (14) Liu, L. Q.; Li, Y.; Zhang, J. G.; Kang, L. M.; Dong, J. B.; Liu, J. Application of multi-parameter flow unit in reservoir evaluation *Journal of Northwest University (Natural Science Edition)* 2009; Vol. 39 01, pp 114–120.
- (15) Song, F.; Yang, S. C.; Sunina; Xiang, K.; Zhao, Y. F.; Cao, H. F. Study on sediment provenance and facies model of the northern margin of the Junggar Basin: A case study of the Chunhui exploration

- area on the front edge of the Hala Alatahan *Acta Sedimentol. Sin.* 2015; Vol. 33 01, pp 49–59.
- (16) Wang, S. Z.; Zhang, K. H.; Jin, Q. Law of blanket-type oil and gas accumulation in the slope zone of the Hashan area at the northern margin of the Junggar Basin *Journal of Xi'an Shiyu University (Natural Science Edition)* 2014; Vol. 25 04, pp 595–602.
- (17) Liu, J. Q. Study on reservoir heterogeneity of the Alrad Oilfield *Neijiang Sci. Technol.* 2019; Vol. 40 02, pp 76–126.
- (18) Zhang, M. S. *Seismic Sedimentology and Its Application in the Xishanyao Formation of the Alade Oilfield*. Master; China University of Petroleum, 2016.
- (19) Choulet, F.; Chen, Y.; Wang, B.; Faure, M.; Cluzel, D.; Charvet, J.; Lin, W.; Xu, B. Late Paleozoic paleogeographic reconstruction of Western Central Asia based upon paleomagnetic data and its geodynamic implications. *J. Asian Earth Sci.* 2011, 42 (5), 867–884, DOI: 10.1016/j.jseas.2010.07.011.
- (20) Mathon, B. R.; Ozbek, M. M.; Pinder, G. F. Transmissivity and storage coefficient estimation by coupling the Cooper–Jacob method and modified fuzzy least-squares regression. *J. Hydrol.* 2008, 353 (3), 267–274.
- (21) Zhang, G. W. Type curve and numerical solutions for estimation of Transmissivity and Storage coefficient with variable discharge condition. *J. Hydrol.* 2013, 476, 345–351.
- (22) Cao, J. Z. Reservoir characteristics and oil and gas accumulation laws of the 6th oil layer group in the Well 79 area of Zibeiyu Oilfield *Doctor Northwest University* 2009.
- (23) Zhang, X.; Yang, D.; Wei, L.; Liu, D.; Li, D. Determining the productivity equation of gas wells using the formation coefficient method *Journal of Xi'an Petroleum University (Natural Science Edition)* 2012; Vol. 27 03, pp 46–49 + 4.
- (24) Pan, Q.; Gao, d.; Li, G.; Zhang, Y. Evaluation and optimization of drill bits using the comprehensive coefficient method of strata *Pet. Drilling Tech.* 2003, 05, pp 36–38.
- (25) Deng, D.; Wang, Y.; Gao, L.; Li, G.; Zhang, J.; Hu, T. Application of Formation Coefficient Method in Production Capacity Prediction of Gas Wells in Su76 Block *Inner Mongolia Petrochem. Ind.* 2021; Vol. 47 02, pp 120–124.
- (26) Deng, D.; Wang, Y.; Lei, G.; Li, G.; Fang, J.; Zhang, J. Predicting gas well productivity in SuX block using improved formation coefficient method *Well Testing* 2021; Vol. 30 03, pp 1–6.
- (27) Center, S. O. B. O. a. G. E. M. *Sedimentary Model and Favorable Reservoir Distribution of the Hasan Chunhui Jurassic Cretaceous System* 2022.
- (28) Yu, L.; Cai, T. Research on the Application of Variable Dynamic Storage Coefficient Method in Flood Routing of the Dalinghe River Basin in Liaoning Province *Jilin Water Resour.* 2013, 09, pp 8–10 + 16.
- (29) Jingzhou, Z.; Shaobo, W.; Fuli, W. On the Classification and Evaluation Standards of Low Permeability Reservoirs: Taking the Ordos Basin as an Example *Lithologic Reservoirs* 2007, 03, pp 28–31 + 53.
- (30) Aslund, B.; Olson, O. T. Testing of laminar air flow units by particle counting and by microbial methods. *Acta Pharm. Suec.* 1976, 13 (5–6), 469–474.
- (31) Mahjour, S. K.; Al-Askari, M. K.; Masihi, M. Identification of flow units using methods of Testerman statistical zonation, flow zone index, and cluster analysis in Tabnaak gas field. *J. Pet. Explor. Production Technol.* 2016, 6 (4), 577–592, DOI: 10.1007/s13202-015-0224-4.
- (32) Mahjour, S. K.; Al-Askari, M. K.; Masihi, M. Identification of Flow-units using Methods of Testerman Statistical Zonation, Flow Zone Index, and Cluster Analysis in Tabnaak Gas Field. *J. Pet. Environ. Biotechnol.* 2015, 6, No. 1000253, DOI: 10.4172/2157-7463.1000253.
- (33) Dai, L.; Zhao, C. Classification and discrimination method of reservoir flow unit index based on Fisher and probability method *Complex Oil Gas Reservoirs* 2021; Vol. 14 02, pp 73–79.
- (34) Jiao, C.; Xu, C. Permeability prediction method based on flow unit index *Logging Technol.* 2006, 04, pp 317–319 + 384.
- (35) Li, C.; Chen, W.; Fu, Y. Using Flow Unit Index for Reservoir Classification and Evaluation *Domestic Foreign Energy Sources* 2012; Vol. 17 10, pp 40–43.
- (36) Song, G.; Li, Z.; Du, Y. Classification and evaluation of reservoir flow units in the 1–5 oil reservoirs of the middle section of the third member of the Shahejie Formation in Pucheng Oilfield *Pet. Geol. Recovery Effic.* 2003, 06, pp 15–17 + 6.
- (37) Changhui, Y.; Dashan, D.; Qing, C. Evaluation of reservoir distribution characteristics using flow unit method *J. Chengdu Inst. Technol.* 2002, 01, pp 37–40.
- (38) Zhao, H. Understanding and Suggestions on the Study of Reservoir Flow Units *Daqing Pet. Geol. Dev.* 2001, 03, pp 8–10 + 74.
- (39) Zhao, C. J.; Jiang, Y. L.; Yang, H. X.; Wang, L. J. The genesis of authigenic minerals and the porosity evolution of various lithologies and their implications for identifying high-quality reservoirs in the fourth member of Xujiahe Formation (Northeast-Sichuan Basin, China). *J. Pet. Sci. Eng.* 2022, 212, No. 110261.
- (40) Yang, W.; Wei, G. Q.; Xie, W. R.; Su, N.; Zen, F. Y.; Hao, C. G.; Bai, Z. Z.; Li, R.; Wu, X. Q.; Su, Y. Q. Main controlling factors and genetic mechanism for the development of high-quality reservoirs in the mound-shoal complexes on the platform margin of the intra-cratonic rift: A case study of the fourth member of the Dengying Formation in the eastern limb of Deyang-Anyue intra-cratonic rift, Sichuan Basin, China. *J. Nat. Gas Geosci.* 2023, 8 (1), 35–48, DOI: 10.1016/j.jnggs.2023.02.001.
- (41) Tao, H. F.; Wang, Q. C.; Yang, X. F.; Jiang, L. Provenance and tectonic setting of Late Carboniferous clastic rocks in West Junggar, Xinjiang, China: A case from the Hala-alat Mountains. *J. Asian Earth Sci.* 2013, 64, 210–222.
- (42) Ma, D. L.; He, D. F.; Li, D.; Tang, J. Y.; Liu, Z. Kinematics of syn-tectonic unconformities and implications for the tectonic evolution of the Hala'alat Mountains at the northwestern margin of the Junggar Basin, Central Asian Orogenic Belt. *Geosci. Front.* 2015, 6 (2), 247–264.
- (43) Yan, D.; Wang, H.; Wang, J.; Wang, Q. Sedimentary Characteristics and Reservoir Prediction of Paleogene in the East Part of Kuqa Foreland Basin. *J. China Univ. Geosci.* 2006, 17 (2), 138–157, DOI: 10.1016/S1002-0705(06)60019-8.
- (44) Leila, M.; Moscariello, A. Seismic stratigraphy and sedimentary facies analysis of the pre- and syn- Messinian salinity crisis sequences, onshore Nile Delta, Egypt: Implications for reservoir quality prediction. *Mar. Pet. Geol.* 2019, 101, 303–321.
- (45) Dou, L. R.; Xu, S. B.; Zhu, Y. H.; Ping, X. C. Genesis and geochemical characteristics of heavy and viscous oil reservoirs in the Eerduosi Basin *Acta Pet. Sin.* 1995, 02, pp 1–7.
- (46) Wang, Y. T.; Diana; Hui, R. Geochemical characteristics and genesis of Permian heavy oil in the northwest margin of the Junggar Basin *Pet. Geol. Exp.* 1997, 02, pp 158–163.
- (47) Zhao, Y. G.; Chen, J. S.; Jiang, Y. Q.; Dong, Z. X.; Zhao, M. H. Reservoir characteristics and controlling factors of the first member of the Shahejie Formation in the Chongzhong Gongshanmiao oilfield *Nat. Gas Explor. Dev.* 2006, 01, pp 10–16+23+79-xs80.
- (48) Han, X. L.; Wu, Q. Q.; Lin, H. X.; Zhang, K. H. Types of oil and gas migration systems and accumulation modes in the Halaar-Altaishan structural belt, northern margin of the Junggar Basin *Nat. Gas Geosci.* 2016; Vol. 27 04, pp 609–618.
- (49) Wang, S. Z.; Zhang, K. H.; Jin, Q. Origin types of crude oil and significance of the Fencheng Formation source rocks in the Harlaarat region of the Junggar Basin *Nat. Gas Geosci.* 2014; Vol. 25 04, pp 595–602.
- (50) Dai, Z. L.; Fan, X. D.; Ma, X. P.; Zhang, X. M. Basic geological characteristics of the Cretaceous Qingshuihe Formation oil sands in the southern margin of the Karamay Basin *Unconv. Oil Gas* 2022; Vol. 9 01, pp 38–47.